IMAGE SIMPLIFICATION BY ROBUST ESTIMATOR BASED RECONSTRUCTION FILTER

Fatih Murat Porikli
Mitsubishi Electric Research Labs,
Murray Hill, NJ 07974, USA,
fatih@merl.com

Abstract

In this contribution, we discuss a robust estimator based on image reconstruction technique for image filtering and simplification purposes. Instead of using the least-squares estimators that the measurement error is independently random and distributed as a normal distribution, a Lorentzian distribution based estimator is employed to fit a model function to the input image within the local windows. The estimator weights the outliers of the measurement inversely with respect to the their deviations unlike the least-squares that magnifies exponentially. We adapted the robust estimator to simplify image by treating image noise and texture as measurement deviations. The results prove that the simplification filters have potential of becoming popular image processing tools.

1 Introduction

Reconstruction of the input data set is in demand recently for estimation problems and data simplification. By leveraging the regularization aspect, the reconstruction works as an independent smoothness constraint in disparity estimation, surface model fitting [1], and optical flow based motion estimation algorithms [2]. Here, we present image reconstruction as an image simplification tool that has several applications ranged from image editing, animation, manipulation, low bitrate object-based compression to segmentation [3]. The modeling of spatial discontinuities [4] for problems such as surface recovery has been intensely studied in computer vision.

The purpose of reconstruction is to remove the texture and noise contaminated in the image such that the edges that generally correspond to the object boundaries are preserved, and the texture within the boundaries are suppressed. It is a smoothing operation that does not smooth the edges. Such a pyramid of simplified images as in Fig. 1 can be employed in a scalable coding technique that adapts content with respect to network constraints. We model the input image in terms of piece-wise linear functions in an iterative framework to obtain simplified image.

In the next section, we explain the robust estimators and their difference from the least-squares based methods. The following section summarizes the image simplification. The test results are included in the conclusions.

2 Image Reconstruction by Robust Estimators

The term robust is, in general, referring to a statistical estimator, it means "insensitive to small departures from the idealized assumptions for which the estimator is optimized." The word small can have two different interpretations, both important: either fractionally small departures for all data points, or else fractionally large departures for a small number of data points. Out of various sorts of robust statistical estimators, we prefer to employ M-estimates that follow from maximum-likelihood arguments. M-estimates are usually the most relevant class for model-fitting, that is, estimation of parameters [5].

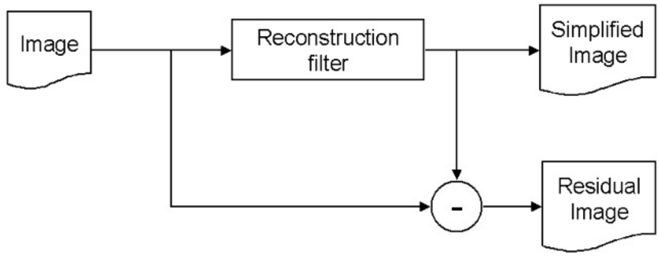

Figure 1: Reconstruction generates filtered and residual images.

Given a set of observations, one often wants to condense and summarize the data by fitting it to a model that depends on adjustable parameters. Suppose that we are fitting N data points $(x_i; y_i)$ $i = 1...N$, to a model that has M adjustable parameters a_j $j = 1...M$. The model predicts a functional relationship between the measured independent and dependent variables,

$$y(x) = y(x; a_1...a_M) \tag{1}$$

where the dependence on the parameters is indicated explicitly on the right-hand side. The first thing that minimize to get fitted value is the familiar least-squares fit,

$$\min_{a_1 \,...\, a_M} \qquad \sum_{i=1}^{N} [y_i - y(x_i; a_1...a_M)]^2 \tag{2}$$

Suppose that each data point y_i has a measurement error that is independently random and distributed as a normal (Gaussian) distribution around the "true" model $y(x)$. And suppose that the standard deviations σ of these normal distributions are the same for all points. Then the probability of the data set is the product of the probabilities of each point,

$$P \propto \prod_{i=1}^{N} \exp\left[-\frac{1}{2}\left(\frac{y_i - y(x_i)}{\sigma}\right)^2\right] \tag{3}$$

Maximizing above equation is equivalent to maximizing its logarithm, or minimizing the negative of its logarithm,

$$\sum_{i=1}^{N} \left(\frac{y_i - y(x_i)}{\sigma}\right)^2 \tag{4}$$

If we take the derivative of the above equation with respect to the parameters a_k, we obtain equations that must hold at the minimum,

$$\sum_{i=1}^{N} \left(\frac{y_i - y(x_i)}{\sigma^2}\right)\left(\frac{\partial y(x_i; a_k)}{\partial a_k}\right) = 0, \qquad k = 1...M. \tag{5}$$

What we see is that least-squares fitting is a maximum likelihood estimation of the fitted parameters if the measurement errors are independent and normally distributed with constant standard deviation.

Suppose we know that our measurement errors are not normally distributed. Then, in deriving a maximum-likelihood formula for the estimated parameters a in a model $y(x;\mathbf{a})$, we would write instead of above equation

$$P \propto \prod_{i=1}^{N} \exp(-\rho(y_i - y(x_i;\mathbf{a}))) \tag{6}$$

where the function ρ is the negative logarithm of the probability density. Taking the logarithm of (6) as above, we find that we want to minimize the expression

$$\sum_{i=1}^{N} \rho(y_i - y(x_i;\mathbf{a})) \tag{7}$$

If we now define the derivative of $\rho(z)$ to be a function $\psi(z)$,

$$\psi(z) \equiv \frac{d\rho(z)}{dz} \tag{8}$$

then the generalization of the case of a general M-estimate is

$$\sum_{i=1}^{N} \frac{1}{\sigma_k}\psi\left(\frac{y_i - y(x_i)}{\sigma_i}\right)\left(\frac{\partial y(x_i;a_k)}{\partial a_k}\right) = 0, \qquad k = 1...M. \tag{9}$$

If we compare (5) to (9), we see at once that the specialization for normally distributed errors is

$$\rho(z) = \frac{1}{2}z^2, \qquad \psi(z) = z. \tag{10}$$

The tails of the Gaussian distribution are exponentially decreasing. A distribution with even more extensive therefore sometimes even more realistic tails is the Cauchy or Lorentzian distribution,

$$P \propto \frac{1}{1 + \frac{1}{2}\left(\frac{y_i - y(x_i)}{\sigma_i}\right)} \tag{11}$$

This implies

$$\rho(z) = \log\left(1 + \frac{1}{2}z^2\right), \qquad \psi(z) = \frac{z}{1 + \frac{1}{2}z^2}. \tag{12}$$

Notice that the $\psi(z)$ function occurs as a weighting function in the generalized normal equations (9). For normally distributed errors, Gaussian distribution says that the more deviant the points, the greater the weight. By contrast, when the tails are even larger as in Lorentzian, the function $\psi(z)$ increases with deviation, then starts decreasing, so that very deviant points the true outliers are not counted at all in the estimation of the parameters.

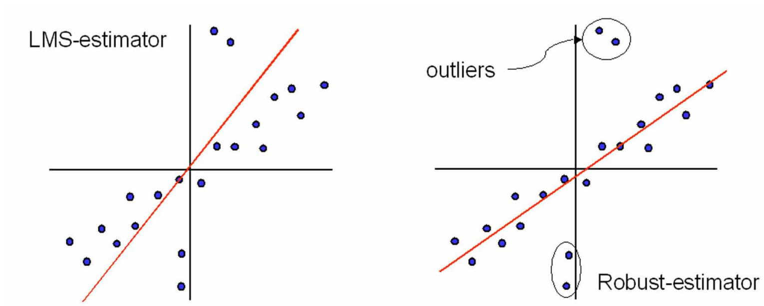

Figure 2: Robust estimator disregards outlier points to find the optimum fit.

3 Image Simplification

Image simplification is a problem of fitting a piece-wise smooth brightness model **u** to image data $I(x, y)$. The assumption of piece-wise smooth brightness is frequently violated in natural images. In textured regions and at intensity boundaries, where the brightness is not uniform, the use of a robust data term allows us to detect and reject the measurements that violate the uniform brightness assumption. Given an image brightness function $I(x, y)$, we want to recover a piece-wise smooth surface **u** that minimizes

$$J(\mathbf{u}, \mathbf{I}) = \sum_{(x,y)\in I} [\rho(u(x, y) - I(x, y), \sigma_D) + \kappa \sum_{(i,j)\in W_{xy}} \rho(u(x, y) - u(i, j), \sigma_S)] \tag{13}$$

where W_{xy} is the window around the point (x, y), and ρ is the Lorentzian. We build simplification filter by using downhill simplex minimization. For every point, a first order function is fit in a local window W. The standard deviations σ_D and σ_S are assumed to be constant for all points. An iterative continuation method is used in which the previously simplified image models u's are used as the observation I of the next iteration. For color imagery, each color band simplified separately. The local window size is adapted to the total iteration number of the algorithm such that for large iteration numbers a small window is chosen. Big iteration numbers and large windows cause more simplified image, e.g., significant amount of reduction in the texture.

4 Conclusions

To compare the simplification results with the other smoothing and noise removal filters, median, low-pass, morphological filters are simulated. A 3×3 median filter that requires 30 comparison per pixels is applied to the test images as shown in Figures 3,4,5-(a). As the low-pass filter, a 2D Gaussian kernel which is computationally similar to the median filter within the 5×5 window is used. Morphological smoothing filter is the concatenated open and closing operators with a 3×3 basic element. However, morphology requires 165 comparisons. Figures 3,4,5-(b) are the median filtered images, and 3,4,5-(c) are the Gaussian filtered results respectively. The morphological filtering results are Figures 3,4,5-(d). The simplified piece-wise constant brightness models that removed a significant amount of the texture contained in the original images are shown in Figures 3,4,5-(e-f). The complexity of the simplification filter is measured in terms of the processing time, and it is observed to be less than the morphological smoothing and similarly performing median filter. A bigger iteration number and a smaller local window size are chosen for the results given in (f)'s in comparison to results in (e)'s. As visible from the results, the robust estimator based simplification filter removes the local texture effectively. It does not smear the edges as the low-pass filter or removes the boundaries as the morphology. Furthermore, it is faster than the median filter.

References

[1] M. Black and A. Rangarajan, "The outlier process: unifying line process and robust statistics", IEEE Conf. on Computer Vision and Pattern Recognition, Seattle, (1994)

[2] M. Black and A. Jepson, "Estimating optical flow in segmented images using variable-order parametric models with local deformations", IEEE Transactions on Pattern Analysis and Machine Intelligence, (1998)

[3] D. Geiger and F. Girosi, "Parallel and deterministic algorithms from MRF's: Surface Reconstruction", IEEE Transactions on Pattern Analysis and Machine Intelligence, (1991)

Figure 3: (a) The original image, (b) median filtered, (c) Gaussian filtered, and (d) morphological smoothed results. (e) The simplified input image within the 5×5 local windows, and (f) simplified within the 3×3 windows iteratively.

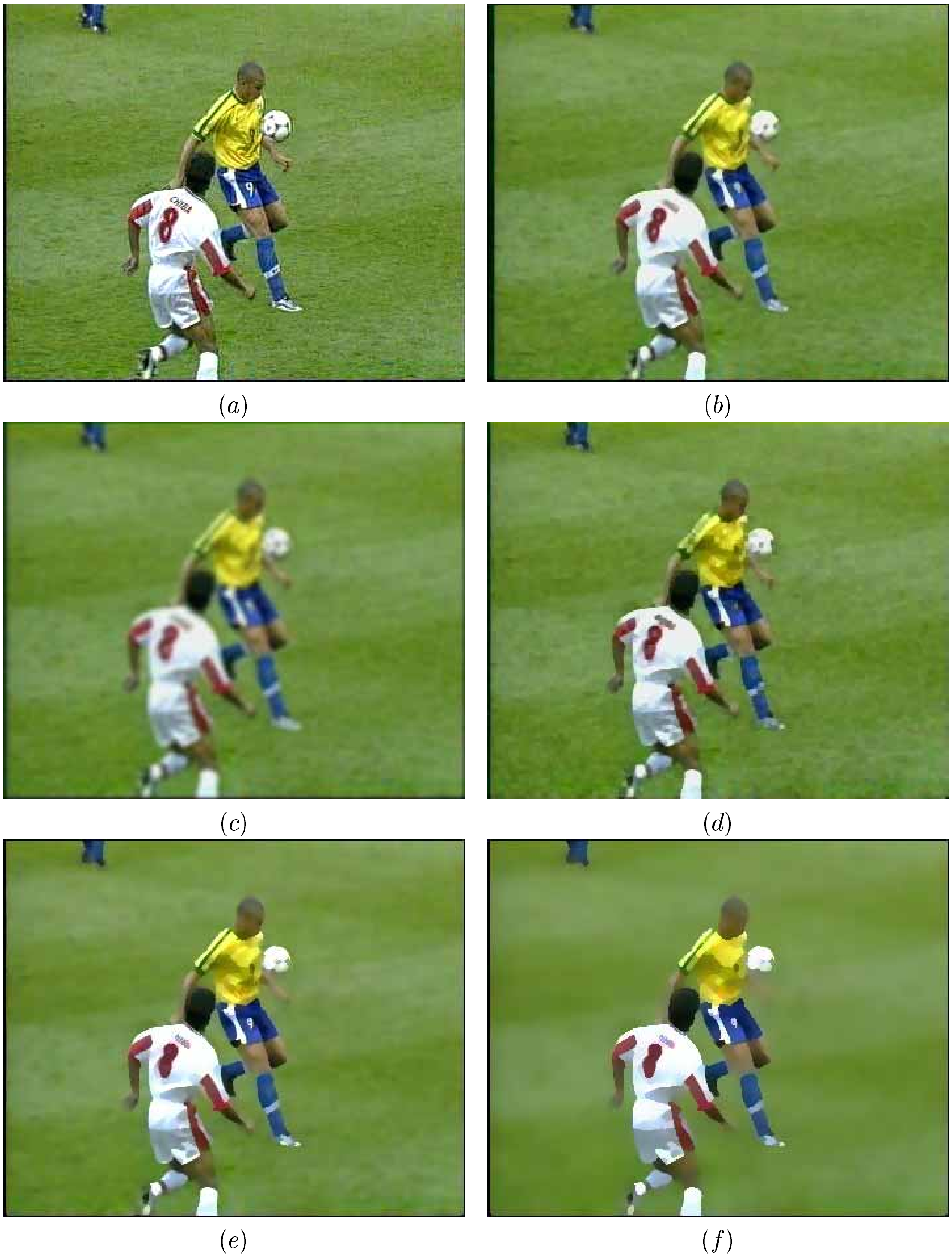

Figure 4: (a) The original image, (b) median filtered, (c) Gaussian filtered, and (d) morphological smoothed results. (e) The simplified input image within the 5×5 local windows, and (f) simplified within the 3×3 windows iteratively.

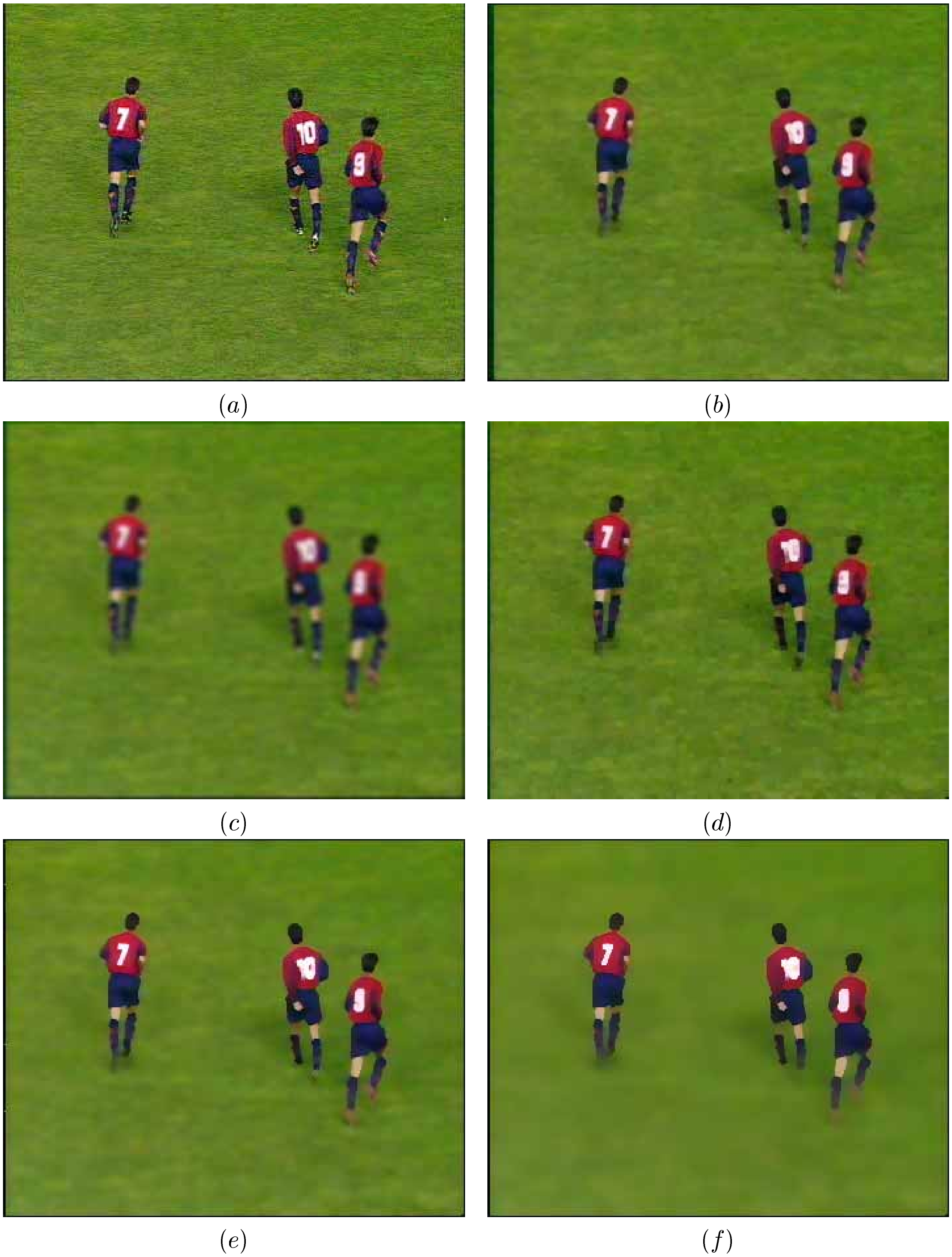

Figure 5: (a) The original image, (b) median filtered, (c) Gaussian filtered, and (d) morphological smoothed results. (e) The simplified input image within the 5×5 local windows, and (f) simplified within the 3×3 windows iteratively.

[4] D. Geman and G. Reynolds, "Constraint reconstruction and recovery of discontinuities", IEEE Transactions on Pattern Analysis and Machine Intelligence, (1992)

[5] F. Hampel, E. Ronchetti, P. Rosseuw, and W. Stahel, "Robust statistics: the approach based on influence functions", John Wiley and Sons, New York, (1986)